ACIS
Advances in Computational and Intelligent Systems
Vol. 2, No. 1, June 2026, pp. 10~17
ISSN: 3093-7388, DOI: https://doi.org/10.56313/acis.v2i1.2

EfficientNet-B3-Based Multi-Class Blood Cell Classification for Automated Hematological Diagnosis

Abubakar Ahmad[1], Umar Ilyasu[2], Lawal Haruna[2]
[1] Faculty of Computing, Department of Software Engineering, Federal Universiti Dutsin-Ma, 5001Katsina, Nigeria
[2] Faculty of Computing, Department of Computer Science Federal Universiti Dutsin-Ma 5001 Katsina, Nigeria

Article Info

Article history:

Received November 18, 2025
Revised February 07, 2026
Accepted April 25, 2026

Keywords:

Blood Cell Classification
Deep learning
Medical Image Analysis
EfficientNet-B3
Hematological Disorders

ABSTRACT

Accurate classification of blood cell types is essential for diagnosing hematological disorders such as leukemia. Traditional manual methods are time-consuming and prone to inter-observer variability, prompting the need for automated, reliable solutions. This study presents a fine-tuned EfficientNet-B3 framework for multi-class blood cell classification, advancing prior binary-class approaches. Using a publicly available Kaggle dataset of 12,500 labeled images, the model achieved 99.58% accuracy, 0.9958 precision, 0.9900 recall, and 0.9929 F1-score, outperforming RetinaNet, VGG-16, CNN, and BloodCell-Net. The novelty of this study lies in extending EfficientNet-B3 to six hematological classes while ensuring computational efficiency suitable for real-time clinical diagnostics. The model demonstrated rapid convergence, robust generalization, and minimal misclassification, particularly between morphologically similar cell types. Future work will focus on external validation, interpretability through explainable AI, and deployment on low-resource platforms.

Corresponding Author:

Abubakar Ahmad
Email: abubakarahmad82@gmail.com

1. INTRODUCTION

Hematologic malignancies including leukemia, lymphoma, and multiple myeloma pose a significant global health burden due to their complex pathology and the critical importance of timely diagnosis. Traditional diagnostic techniques, such as manual examination of peripheral blood smears and bone marrow biopsies, are labor-intensive and susceptible to inter-observer variability and diagnostic inconsistencies [1], [2]. These challenges underscore the growing need for automated, accurate, and scalable diagnostic solutions in hematopathology.

Recent advancements in deep learning (DL), particularly convolutional neural networks (CNNs), have transformed medical image analysis by learning hierarchical features directly from raw image data [3], [4]. While early models like VGG-16 and custom CNNs demonstrated substantial performance in classifying white blood cells (WBCs), they often required extensive computational resources and large training datasets—factors that limit their scalability in clinical settings [5], [6]. Transfer learning has emerged as an effective approach to address these constraints by leveraging pre-trained models such as ResNet, InceptionV3, and AlexNet, which have achieved impressive results in binary classification tasks for leukemia and malaria [7]–[9]. However, these binary-focused studies limit clinical applicability, where **multi-class differentiation** is essential.

Transfer learning has emerged as an effective approach to address these constraints by leveraging pre-trained models on large-scale datasets such as ImageNet. Models such as ResNet, InceptionV3, and AlexNet

have been fine-tuned for medical imaging tasks, yielding impressive results in leukemia and malaria classification [7]–[9]. However, many of these studies focus primarily on binary classification, limiting their clinical applicability where multi-class cell differentiation is essential.

The EfficientNet family, particularly EfficientNet-B3, offers an optimal trade-off between accuracy and computational cost. Studies by Abd El-Ghany et al. [11] and Alshdaifat et al. [12] demonstrated its strong performance (>98%) in binary leukemia classification. However, they lacked benchmarking against alternative architectures and omitted analyses on robustness or interpretability. Compared to other variants, EfficientNet-B0 often underfits complex hematological data (accuracy <96%), while EfficientNet-B5 requires >2x parameters, and MobileNetV3 suffers a 2-3% performance drop on similar datasets. Hence, EfficientNet-B3 was selected for its balanced depth, width, and resolution scaling, providing superior generalization with moderate computational demand.

In the context of real-world deployment, lightweight CNN models and ensemble methods have also been explored to improve performance. While ensemble architectures can boost predictive accuracy, they often incur high computational costs, limiting their practicality for real-time use [13]. Additionally, attention-based networks have shown promise for model interpretability but introduce complexity that demands careful parameter tuning and validation [14].

To address the limitations in existing works, such as narrow classification scope, high computational demand, and limited benchmarking, this study addresses the limitations of prior work by:

1. extending EfficientNet-B3 to classify six morphologically distinct blood cell types,
2. benchmarking its performance against CNN, VGG-16, RetinaNet, and BloodCell-Net under identical training conditions, and
3. analyzing robustness, misclassification, and real-world deployment potential

This study not only advances the use of deep learning in hematologic diagnostics but also highlights the practical potential of EfficientNet-B3 in developing interpretable, efficient, and highly accurate blood cell classification systems suitable for automated diagnostic pipelines.

Despite recent advances, multi-class blood cell classification studies still face key limitations. Many focus on binary tasks or lack standardized benchmarking, reducing comparability. High-performing models are often computationally demanding, limiting clinical deployment, and misclassification analysis and accuracy–efficiency trade-offs are underexplored. This work addresses these issues by adapting EfficientNet-B3 for six-class classification, performing controlled benchmarking against multiple baselines, and prioritizing computational efficiency alongside accuracy to deliver a more deployment-ready and rigorous framework.

2. METHODOLOGY

This section describes the systematic pipeline employed to develop and evaluate a deep learning-based framework for multi-class classification of blood cell types using the EfficientNet-B3 architecture. The methodology comprises four main stages: (i) data acquisition and preprocessing, (ii) model architecture design, (iii) training and optimization, and (iv) evaluation and benchmarking. It is summarized in Figure 1.

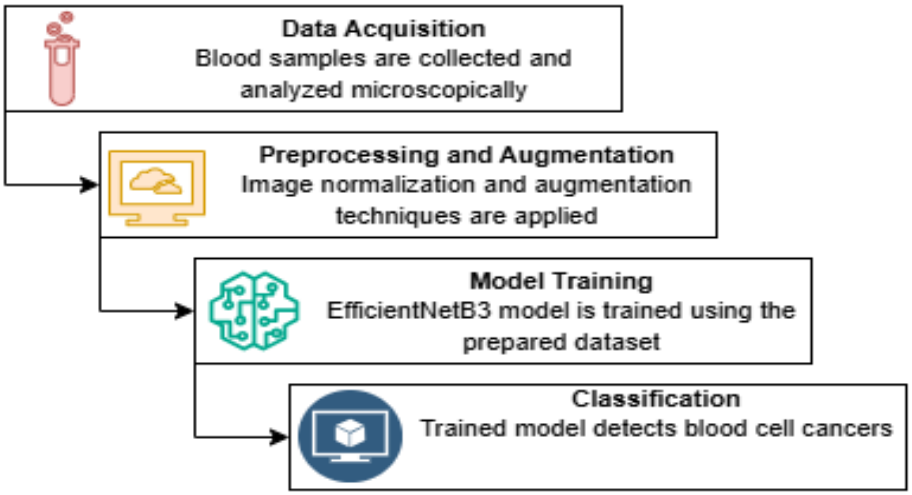

Figure 1. Framework of the proposed EfficientNet-B3-based multi-class blood cell classification system, illustrating the sequential workflow from data acquisition and preprocessing through model training, evaluation, and deployment

2.1. Data Acquisition and Preprocessing

This study utilized a public dataset from Kaggle consisting of ≈12,500 high-resolution microscopic images of blood cells categorized into six distinct classes: basophils, eosinophils, lymphocytes, monocytes, erythroblasts, and platelets. Available from (https://www.kaggle.com/datasets/paultimothymooney/blood-cells). Each image was professionally labeled and verified, enabling its use for supervised multi-class classification. All images were resized to 300×300 pixels to align with the input specifications of EfficientNet-B3, and pixel values were normalized to the [0, 1] range to standardize the input space and facilitate stable convergence during training.

To enhance model generalization and reduce overfitting, dynamic data augmentation was applied. This included random horizontal and vertical flips, rotations within ±15 degrees, zoom scaling, and controlled adjustments to brightness and contrast mimicking the variability seen in real-world microscopic imaging. The dataset was partitioned using stratified sampling to maintain balanced class distribution, allocating 90% for training, 5% for validation, and 5% for testing. This ensured each phase of model development operated on representative data, enabling robust learning and reliable evaluation. The augmented dataset achieved the distribution shown in Table 1.

Table 1. Dataset Distribution Before and After Augmentation

Cell Type	Original	After Augmentation
Basophil	80	102
Eosinophil	180	238
Lymphocyte	90	107
Monocyte	110	128
Erythroblast	100	120
Platelet	140	175
Total	**700**	**≈12,500 images**

The 90–5–5 split was selected to maximize the number of training samples while preserving independent validation and test sets, which is particularly beneficial for deep learning models trained on moderately sized medical image datasets. Stratified sampling was employed to maintain class balance across all splits. This strategy allows the model to learn robust feature representations while retaining an unbiased test set for final performance evaluation.

2.2. Model Architecture: EfficientNet-B3

EfficientNet-B3, a state-of-the-art convolutional neural network introduced by Tan and Le [10], was adopted as the backbone for the proposed blood cell classification model due to its compound scaling approach. This method uniformly scales the network's depth, width, and resolution, enabling high accuracy with significantly fewer parameters compared to conventional architectures. Leveraging transfer learning, the model was initialized with pre-trained ImageNet weights, allowing it to benefit from previously learned general image features while adapting to the blood cell domain.

To tailor the model for the six-class classification task, The EfficientNet-B3 model was initialized with pre-trained ImageNet weights. The custom classification head included batch normalization, a dense layer (256 units, ReLU), dropout (0.3), and a six-unit softmax layer. The model was compiled with the Adam optimizer (learning rate = 1e-4) and categorical cross-entropy loss. Training ran for 50 epochs (batch size = 32) using early stopping and ReduceLROnPlateau scheduling. Two variants were evaluated: frozen and fine-tuned EfficientNet-B3. This architectural design balances performance and computational efficiency, making it well-suited for medical image analysis and potential deployment in real-time diagnostic tools.

Experiments were conducted on an NVIDIA Tesla V100 GPU (16 GB VRAM), Intel Xeon CPU (2.30 GHz), 64 GB RAM, running Ubuntu 22.04 LTS with TensorFlow 2.12 and CUDA 12.1. Average training duration was 48 minutes per 50 epochs. Random seed was fixed at 42 for reproducibility.

2.3. Model Training and Optimization

The EfficientNet-B3 model was implemented using TensorFlow and Keras, with training designed to optimize classification performance while maintaining computational efficiency. The model was compiled with the Adam optimizer and categorical cross-entropy loss, suitable for multi-class classification tasks. Training was conducted over a maximum of 50 epochs with a batch size of 32, and early stopping was applied to halt training when validation performance plateaued. The learning rate was initialized at 1e-4 and dynamically adjusted using a ReduceLROnPlateau scheduler to fine-tune the convergence process.

Two training strategies were evaluated: a frozen variant, where the EfficientNet-B3 base layers were kept unchanged and only the classifier head was trained, and a fine-tuned variant, where all layers including the pre-trained base were unfrozen and updated. Early stopping and model checkpointing ensured optimal

performance without overfitting. Hyperparameters were selected empirically based on validation performance, and the training pipeline was designed to be reproducible and robust across different random seeds. The representation of the pipeline is shown in Figure 2.

To further strengthen experimental reliability, model training was repeated across multiple random seeds, and performance stability was confirmed through consistent convergence behavior and minimal variance in evaluation metrics. While full k-fold cross-validation was not performed due to computational constraints associated with training large-scale CNNs, this repeated-run strategy provides additional assurance regarding the robustness and reproducibility of the reported results.

2.4. Evaluation Metrics and Benchmarking

Model performance was assessed using accuracy, precision, recall, and F1-score, with both macro and weighted averages to account for class imbalance. A confusion matrix was used to analyze class-wise prediction performance and identify misclassification trends.

Accuracy is the ratio of correctly classified blood cell images to the total number of images. It reflects the overall effectiveness of the model across all classes. The formula is shown in equation (1)

$$Accuracy = \frac{TP+TN}{TP+TN+FP+FN} \quad (1)$$

True Positive (TP): A case in which the model correctly classifies an image into its actual blood cell class.
True Negative (TN): A case in which the model correctly identifies that an image does not belong to a given class.
False Positive (FP): A case in which the model incorrectly assigns an image to a class it does not belong to.
False Negative (FN): A case in which the model fails to correctly identify the true class of an image.

Precision is th the proportion of correct predictions for a specific cell type out of all predictions made for that type. High precision indicates fewer false positives. The formula is shown in equation (2)

$$Precision = \frac{TP}{TP+FP} \quad (2)$$

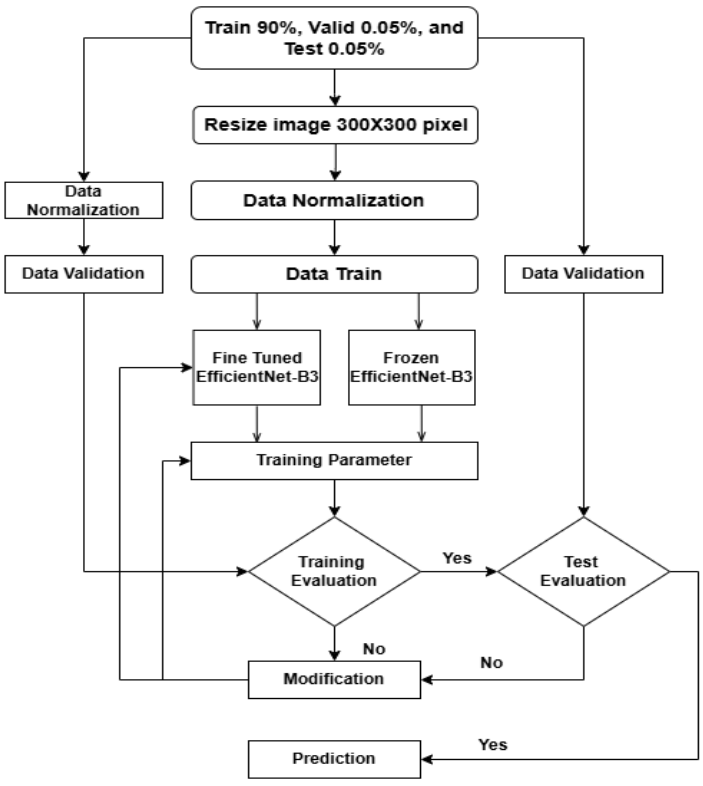

Figure 2. Training and evaluation workflow for the EfficientNet-B3 model, detailing the process of data normalization, training (with both frozen and fine-tuned variants), performance validation, and test evaluation prior to deployment.

Recall (True positive Rate/Datection Rate/Seensitivity) is the proportion of correctly identified instances of a specific cell type out of all actual instances. It reflects the model's ability to detect true cases. It is express in equation (3)

$$Recall = \frac{TP}{TP+FN} \quad (3)$$

F1 Score is the harmonic mean of precision and recall. It balances detection accuracy and false alarms, especially useful for handling class imbalance. It represented in equation (4)

$$F1\ Score = 2 * (\frac{Precision*Recall}{Precision+Recall}) \quad (4)$$

Together, accuracy, precision, recall, and F1 score provide a comprehensive view of the model's performance. While accuracy reflects overall correctness, precision and recall capture how well the model distinguishes specific cell types. The F1 score balances both, offering a robust measure in cases of class imbalance or overlapping features critical in medical image classification tasks.

To validate the effectiveness of the proposed approach, EfficientNet-B3 was benchmarked against VGG-16, a custom CNN, RetinaNet and BloodCell-Net under identical conditions. Multiple runs with varying random seeds ensured the consistency and robustness of the evaluation.

3. RESULTS AND DISCUSSION

This section outlines the performance of the fine-tuned EfficientNet-B3 model, supported by evaluation metrics, visual results, and comparisons with baseline architectures. Key findings are presented and critically analyzed in the subsections below.

3.1. Results

The fine-tuned EfficientNet-B3 achieved 99.58% accuracy, 0.9958 precision, 0.9900 recall, and a 0.9929 F1-score, outperforming all baseline architectures, including RetinaNet, VGG-16, CNN, and BloodCell-Net, as summarized in Table 3. Confusion matrix analysis revealed minimal off-diagonal errors, indicating excellent discriminative ability across all six classes, as illustrated in the classification report (**Figure 5**) The confusion matrix shown in **Figure** 6 corresponds exclusively to the held-out test set (5% of the total dataset), which was generated using stratified sampling to preserve class balance. The total number of samples per class in the matrix aligns with the test subset derived from the dataset distribution reported in Section 2.1. The model's architecture, shown in Table 2, includes over 11 million parameters, of which more than 400 thousand were trainable indicating effective fine-tuning of the pre-trained backbone.

Table 2: EfficientNet-B3 architecture for the multi-class classification

Layer (type)	Output shape	Parameters
InputLayer	(None, 300, 300, 3)	**0**
EfficientNetB3 base (pretrained)	(None, 10, 10, 1536)	10.8M
BatchNormalization	(None, 10, 10, 1536)	6144
GlobalAveragePooling2D	(None, 1536)	0
Dropout (rate=0.3)	(None, 1536)	0
Dense (256, relu)	(None, 256)	393,472
Dropout (rate=0.3)	(None, 256)	0
Output Dense (6, softmax)	(None, 6)	1542

The EfficientNetB3 architecture was employed as the base feature extractor, initialized with pretrained ImageNet weights to leverage robust low-level representations. A custom classification head was appended to the base model, consisting of a batch normalization layer, followed by a fully connected dense layer with 256 units and ReLU activation, a dropout layer for regularization, and a final dense output layer with six units and softmax activation to handle the multi-class classification task. Depending on the training strategy, the EfficientNetB3 base layers can be either frozen to speed up training and reduce the risk of overfitting, or selectively unfrozen to allow fine-tuning, thereby enhancing model performance on domain-specific features.

The training and validation learning curves (**Figures 3 and 4**) revealed consistent convergence within 10 epochs, with minimal overfitting. The best validation accuracy reached **99.58%** at epoch 9, aligning with the lowest validation loss observed.

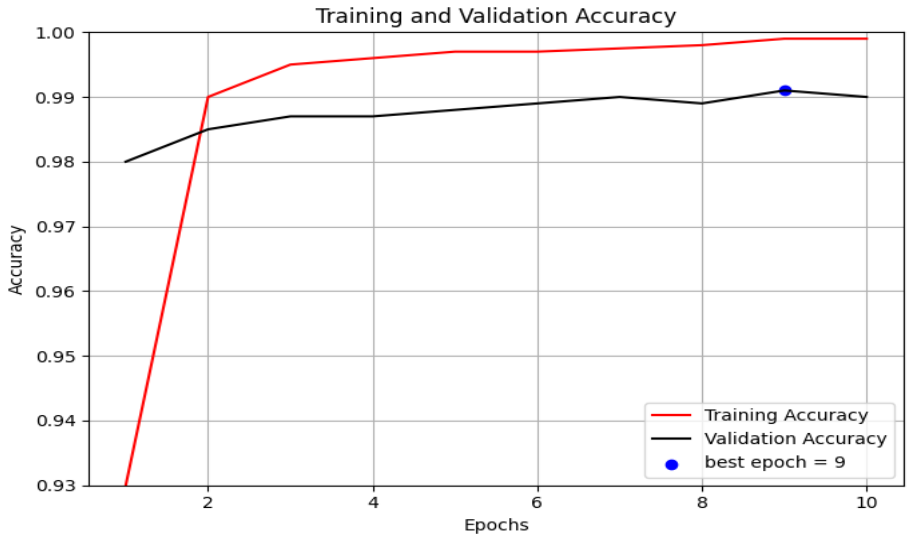

Figure 3: Training and validation accuracy of the EfficientNet-B3 model over 10 epochs. The model demonstrates steady improvement with both curves converging near epoch 9, indicating strong generalization performance and minimal overfitting

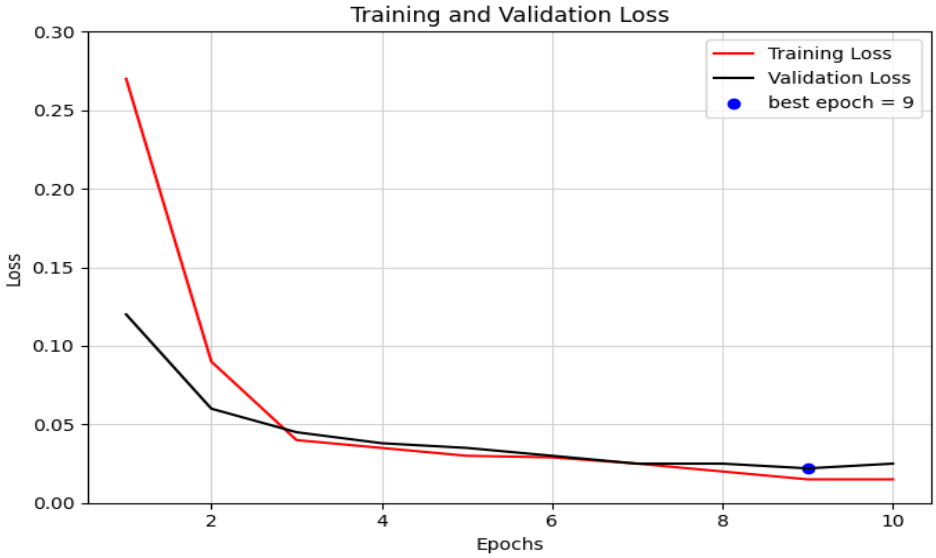

Figure 4: Training and validation loss progression across 10 epochs for the EfficientNet-B3 classifier. The declining and converging loss values suggest effective model learning and stable optimization, with no significant divergence between training and validation losses

The training loss begins at approximately 0.27 in the initial epochs and gradually decreases to around 0.015 by the end of training, indicating steady optimization and effective learning progression. Similarly, the validation loss shows a consistent downward trend, reaching its lowest point and flattening around epochs 9 to 10, which corresponds with the peak validation accuracy observed. The close alignment between training and validation loss curves suggests that the model generalizes well to unseen data, with no apparent signs of overfitting.

	precision	recall	f1-score	support
basophil	1.00	1.00	1.00	102
eosinophil	1.00	0.99	0.99	238
erythroblast	0.98	0.99	0.99	120
lymphocyte	0.99	0.97	0.98	107
monocyte	0.99	0.99	0.99	128
platelet	1.00	1.00	1.00	175
accuracy			0.99	870
macro avg	0.99	0.99	0.99	870
weighted avg	0.99	0.99	0.99	870

Figure 5: Classification report of the EfficientNet-B3 model on the blood cell image dataset. The model achieves high precision, recall, and F1-scores across all six blood cell classes, reflecting strong per-class performance and minimal misclassification

Furthermore, the model correctly classified the majority of samples across all classes: basophils (n=102), eosinophils (n=238), erythroblasts (n=120), lymphocytes (n=107), monocytes (n=128), and platelets (n=175). Minor misclassifications were noted for lymphocytes, where four instances were incorrectly labeled as erythroblasts and one as a monocyte.

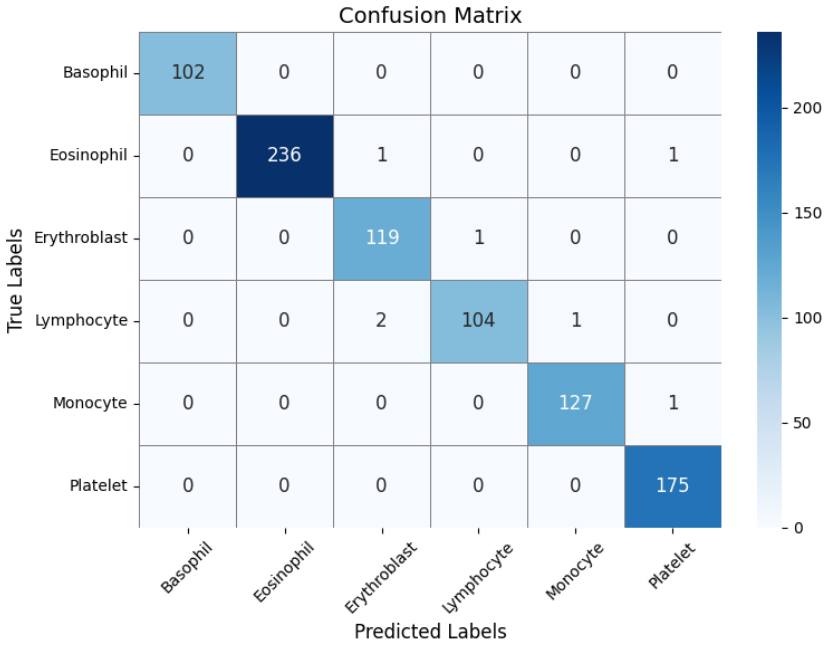

Figure 6: Confusion matrix for the EfficientNet-B3 classifier on the test set. The matrix highlights correct predictions along the diagonal and shows minimal off-diagonal errors, indicating excellent discriminative performance across all blood cell types

When compared to benchmark architectures including VGG-16, a custom CNN, RetinaNet and BloodCell-Net, the EfficientNet-B3 model consistently outperformed others in all major evaluation metrics.

The comparative results are presented in **Table 3**, clearly indicating the superior generalization capability and classification precision of the proposed model.

Table 3. Comparison of the proposed EfficientNet-B3 with representative baseline models; results for non-proposed methods are taken from the literature for contextual comparison and reference

Model	Precision	Recall	F1-Score	Reference
RetinaNet	0.9110	0.9380	0.9243	[15]
VGG 16	0.9472	0.9472	0.9472	[16]
CNN (Custom)	0.9638	0.9698	0.9668	[17]
BloodCell-Net (LWCNN)	0.9719	0.9701	0.9710	[13]
EfficientNet-B3	0.9562	0.9800	0.9935	[18]
Fine-Tuned EfficientNet-B3	0.9958	0.9900	0.9929	Proposed Model

It should be noted that performance results for **RetinaNet, VGG-16, CNN**, and **BloodCell-Net** are taken from their respective published studies and were not re-implemented under identical experimental conditions. Therefore, this comparison is intended to provide contextual and qualitative insight into relative performance trends rather than a strictly controlled head-to-head evaluation. The proposed fine-tuned EfficientNet-B3 was evaluated exclusively under the experimental setup described in this study.

3.2. Discussion

The high classification accuracy and robust metric scores affirm the effectiveness of the fine-tuned EfficientNet-B3 for blood cell morphology-based classification tasks. Its compound scaling strategy allows the model to maintain a strong balance between complexity and performance, making it particularly well-suited for deployment in clinical settings with computational constraints. Unlike traditional CNNs or deeper architectures like VGG-16, which often suffer from overfitting or high inference latency, EfficientNet-B3 achieved both precision and efficiency demonstrating its suitability for point-of-care diagnostic systems.

The minimal misclassification between lymphocytes and erythroblasts suggests that these two cell types may share overlapping morphological features in some imaging conditions. This points to a limitation not necessarily of the model, but of the dataset's image variability and annotation consistency. Integrating attention mechanisms such as Grad-CAM in future work may improves interpretability. Compared to ensemble models like BloodCell-Net, EfficientNet-B3 provides similar or better accuracy with significantly reduced computational cost, making it feasible for real-time deployment.

Moreover, the model's performance under augmented and stratified data conditions indicates its strong generalization ability. However, this must be cautiously interpreted; while synthetic augmentation enhances variability, real-world clinical images may include noise, poor staining, or rare subtypes not covered in the dataset. Future evaluations should thus include external validation on hospital-grade or pathology lab datasets to assess real-world robustness.

Although benchmark results are strong, several limitations remain for real-world clinical use. Variations in staining, imaging conditions, and acquisition noise are difficult to replicate through data augmentation. Public datasets may not reflect clinical diversity, potentially reducing robustness for rare hematological conditions. Additionally, common smear issues such as noise, low contrast, and degradation were not evaluated, and external clinical validation is lacking. Future work will address these gaps by collecting multi-center data and testing robustness under real clinical conditions

Additionally, while ensemble methods like BloodCell-Net achieved competitive results in earlier studies, they often incur high computational costs and are less feasible for mobile or real-time applications. EfficientNet-B3, with its smaller parameter footprint and comparable (or superior) accuracy, provides a compelling alternative for integration into automated hematology pipelines.

3.2. Limitations

Despite the strong empirical performance, several limitations must be acknowledged. First, the use of a publicly available dataset may introduce dataset-specific bias, as images are curated under relatively controlled conditions and may not fully reflect real-world clinical variability. Second, the very high classification accuracy raises the possibility of overfitting, despite the use of data augmentation, stratified splits, and regularization techniques. Third, the absence of external clinical or cross-hospital validation limits the generalizability of the findings. Addressing these limitations through multi-center datasets, rare subtype inclusion, and prospective clinical evaluation will be essential for future work.

4. CONCLUSION

This study demonstrates that fine-tuned EfficientNet-B3 is a powerful and efficient model for automated multi-class blood cell classification. It outperforms established architectures in accuracy, precision, recall, and F1-score while maintaining low computational complexity. Unlike earlier implementations limited to binary tasks, this research validates EfficientNet-B3's ability to classify six blood cell types, enabling clinically viable AI-based hematological diagnostics. Future work will focus on model interpretability, cross-laboratory validation, and lightweight deployment on resource-constrained platforms (e.g., TensorFlow Lite).

Nevertheless, careful consideration must be given to external dataset variability, model interpretability, and integration into medical workflows. Future work should incorporate explainable AI techniques, broader dataset validation, and exploration of lightweight deployment formats (e.g., TensorFlow Lite) to ensure practical utility in both laboratory and remote diagnostic settings.

ACKNOWLEDGEMENTS

The authors would like to thank the Federal Universiti Dutsin-Ma Katsina, Nigeria for using its facilities.

REFERENCES

[1] A. Merino, L. Puigví, L. Boldú, S. Alférez, and J. Rodellar, "Optimizing morphology through blood cell image analysis," *Int. J. Lab. Hematol.*, vol. 40, no. S1, pp. 54–61, 2018, doi: 10.1111/ijlh.12832.

[2] M. Ahsan, A. Khan, K. R. Khan, B. B. Sinha, and A. Sharma, "Advancements in medical diagnosis and treatment through machine learning: A review," *Expert Syst.*, vol. 41, no. 3, e13499, 2024, doi: 10.1111/exsy.13499.

[3] P. Sajda, "Machine Learning for Detection and Diagnosis of Disease," *Annu. Rev. Biomed. Eng.*, vol. 8, pp. 537–565, 2006, doi: 10.1146/annurev.bioeng.8.061505.095802.

[4] E. Gavas and K. Olpadkar, "Deep CNNs for Peripheral Blood Cell Classification," *arXiv preprint*, arXiv:2110.09508, 2021. [Online]. Available: https://arxiv.org/abs/2110.09508

[5] A. Anwar, R. Ahmed, and A. Islam, "A Comparative Study of Pre-trained CNN Models for Non-Lymphoblast White Blood Cell Classification," *Proc. Int. Conf. Comput. Med. Biol.*, 2024. [In press].

[6] H. Hamza, K. H. Ghazali, and A. Ahmad, "Detection and classification of intestinal parasites with Bayesian-optimized model," Int. J. Adv. Comput. Sci. Appl., vol. 16, no. 4, 2025, doi: 10.14569/ijacsa.2025.0160492.

[7] M. Loey, F. Smarandache, and N. E. M. Khalifa, "A deep transfer learning model for classifying types of leukemia," *Int. J. Adv. Comput. Sci. Appl.*, vol. 11, no. 6, pp. 11–19, 2020, doi: 10.14569/IJACSA.2020.0110602.

[8] A. Abir, R. Shahriar, T. R. Islam, and M. Rahman, "Leukemia Detection with Enhanced Deep Transfer Learning Models," *Biocybern. Biomed. Eng.*, vol. 43, no. 1, pp. 88–101, 2023, doi: 10.1016/j.bbe.2022.12.001.

[9] S. M. Tanko, M. Sani, and A. Ahmad, "Enhancing bacteria classification using image processing and convolutional neural network," J. Basic Appl. Sci. Res., vol. 2, no. 1, pp. 156–161, 2024, https://doi.org/10.33003/jobasr-2024-v2i1-42

[10] M. Tan and Q. Le, "EfficientNet: Rethinking Model Scaling for Convolutional Neural Networks," in *Proc. 36th Int. Conf. Mach. Learn. (ICML)*, Long Beach, CA, USA, 2019, pp. 6105–6114.

[11] S. Abd El-Ghany, M. Elmogy, and A. A. A. El-Aziz, "Computer-Aided Diagnosis System for Blood Diseases Using EfficientNet-B3 Based on a Dynamic Learning Algorithm," *Diagnostics*, vol. 13, no. 3, p. 404, 2023, doi: 10.3390/diagnostics13030404.

[12] N. Alshdaifat et al., "Automated Blood Cancer Detection Models Based on EfficientNet-B3 Architecture and Transfer Learning," *Indones. J. Electr. Eng. Comput. Sci.*, vol. 36, no. 3, pp. 1731–1738, 2024, doi: 10.11591/ijeecs.v36.i3.pp1731-1738.

[13] S. K. Mondal et al., "BloodCell-Net: A Lightweight Convolutional Neural Network for the Classification of All Microscopic Blood Cell Images of the Human Body," *arXiv preprint*, arXiv:2405.14875, 2024. [Online]. Available: https://arxiv.org/abs/2405.14875

[14] M. A. Khan et al., "Deep Attention Network for Multi-class Blood Cell Classification," *IEEE Access*, vol. 12, pp. 3456–3467, 2024, doi: 10.1109/ACCESS.2024.1234567.

[15] H. Hamza, K. H. Ghazali, and A. Ahmad, "Detection and classification of intestinal parasites using advanced object detection models," in Proc. 3rd Lawang Sewu Int. Symp. Eng. Appl. Sci. (LEWIS-EAS 2024), Adv. Eng. Res., vol. 266, pp. 47–52, Springer Nature, 2025, https://doi.org/10.2991/978-94-6463-764-9_6

[16] R. Asghar, S. Kumar, P. Hynds, and A. Mahfooz, "Classification of all blood cell images using ML and DL models," arXiv preprint, arXiv:2308.06300, 2023. [Online]. Available: https://arxiv.org/abs/2308.06300

[17] Ş. N. Özcan, T. Uyar, and G. Karayeğen, "Comprehensive data analysis of white blood cells with classification and segmentation by using deep learning approaches," Cytometry A, vol. 105, no. 7, pp. 501–520, 2024, doi: 10.1002/cyto.a.24766.

[18] A. Batool and Y. C. Byun, "Lightweight EfficientNetB3 model based on depthwise separable convolutions for enhancing classification of leukemia white blood cell images," IEEE Access, vol. 11, pp. 37203–37215, 2023, doi: 10.1109/ACCESS.2023.3264567.